Different masking effects on "hole" and "no-hole" figures

Junjun Zhang
Lab of Mind, Art & Computation, Xiamen University, Xiamen, China

Weina Zhu
Lab Mind, Art & Computation, Xiamen University, Kunming Inst Zoology, Chinese Academy Sciences, State Key Laboratory Brain & Cognitive Science, Inst Biophysics, Chinese Academy Sciences, Beijing, Dept Computer Science, Yunnan University, Kunming, China

Xiaojun Ding
Lab of Mind, Art & Computation, Xiamen University, Xiamen, China

Changle Zhou
Lab of Mind, Art & Computation, Xiamen University, Xiamen, China

Xintian Hu
Kunming Institute of Zoology, Chinese Academy of Sciences, Kunming, China, & State Key Laboratory of Brain and Cognitive Science, Institute of Biophysics, Chinese Academy of Sciences, Beijing, China

Yuanye Ma
Kunming Institute of Zoology, Chinese Academy of Sciences, Kunming, China, & State Key Laboratory of Brain and Cognitive Science, Institute of Biophysics, Chinese Academy of Sciences, Beijing, China

Global information is considered the primitive of visual perception in Gestalt psychology. Further, L. Chen (2005) proposed a new theory of topological visual perception. According to this theory, the perception of topological difference is faster than other feature differences. However, it is still not clear why topological perception has the priority. Based on previous studies, we hypothesize that it is caused by the different perception between figures with "hole" and figures without "hole" in the primitive of vision. In the present paper, four behavioral experiments and one ERP experiment were presented. Four behavioral experiments utilizing backward masking paradigm demonstrated that under the same masking effect, "hole" was easier perceived than "no hole". The ERP data may suggest that feedback connection in visual ventral pathway is disturbed by backward masking for "no-hole" stimuli, while it almost remains the same for "hole" stimuli. We suggest that temporal visual cortex is sensitive to "hole", thus facilitating the feedback connection to the occipital cortex. That is one of the reasons why topological perception is prior to local perception.

Keywords: evoked potentials, masking, perceptual organization, object recognition, texture

Citation: Zhang, J., Zhu, W., Ding, X., Zhou, C., Hu, X., & Ma, Y. (2009). Different masking effects on "hole" and "no-hole" figures. *Journal of Vision, 9*(9):6, 1–14, http://journalofvision.org/9/9/6/, doi:10.1167/9.9.6.

Introduction

One of the fundamental questions of vision is the primitive of visual perception. In Gestalt psychology, as indicated by the conception of perceptual organization, the perceptual processing is from global to local, so the primitive of visual perception is to process global information. However, the Gestalt laws for perceptual organization are somehow casual and subjective (Pomerantz, 2003). Explicitly, Chen (1982) proposed a topological approach to perceptual organization. According to the theory, topological property, as a global property, is the primitive of visual perception, and figures with topological differences can be discriminated easier than figures with local feature differences (Chen, 2005; Chen, Zhang, & Srinivasan, 2003; Wang, Zhou, Zhuo, & Chen, 2007; Zhuo et al., 2003). It is worthwhile to investigate what causes the topological

doi: 10.1167/9.9.6 Received April 15, 2009; published August 17, 2009 ISSN 1534-7362

differences. Mostly, topological perception is generated by comparing figures with different number of holes, especially with figures with a hole and figures without any holes. So, it may imply that the priority of topological perception is caused because the perception to "hole" and "no hole" is different at the primitive of visual perception. Another unit recording study on monkey conducted by Komatsu and Ideura (1993) may support this possibility. In their result, a neuron in inferior temporal (IT) cortex was found to be selectively activated by "hole" in a short latency before 100 ms. In addition, in Chen's fMRI results (Wang et al., 2007; Zhuo et al., 2003), rather than primary visual cortex, anterior temporal lobe was activated during topological perception. Furthermore, a behavioral study on amblyopes carried out in our laboratory showed that the perception of visual local features is interfered on amblyopic subjects, while topological perception is intact (Ren et al., 2007). This result indicated that V1 is not crucial for topological perception. Taking together, we have reason to suspect that temporal area is sensitive to "hole" in the primitive of visual perception. Temporal area responded strongly to "hole" than "no hole", thus result in the different perceptions on "hole" and "no hole".

Intuitively, hole can be understood in this way: within a figure, there is an area surrounded by this figure and is homogeneous with the background, such as the same color or the same texture. Casati (2009) gave a more practical definition: to detect a hole, one must first detect a maximal uniform connected unit (figure) and then calculate the numbers of complete visual boundaries of the unit. A hole means a unit with two boundaries; no hole means a unit with only one boundary. There is still a lack of psychological or physiological data to support the idea whether "hole" itself is a primitive visual feature, or "unit" and "complete boundary" are the primitive visual features. However, "hole", "unit", and "complete boundary" are all global features. Compared to primary visual cortex, the size of receptive fields in higher visual cortex is larger. So it also suggests that if there is an area sensitive to "hole" or related global features, it should be higher visual cortex, rather than primary visual cortex.

At the primitive of visual perception, the fundamental task is to segment figures from their background (Haynes, Driver, & Rees, 2005; Heinen, Jolij, & Lamme, 2005; Scholte, Jolij, Fahrenfort, & Lamme, 2008; Thielscher, Kölle, Neumann, Spitzer, & Grön, 2008). According to Chen's theory, it is topological invariance to segregate figure from its background. Therefore, it is probably different to segregate "hole" and "no hole" from their background. Figure–ground segmentation consists of two processes: boundary detection and subsequent surface segregation (Altmann, Bülthoff, & Kourtzi, 2003; Appelbaum, Wade, Vildavski, Pettet, & Norcia, 2006; Bach & Meigen, 1992; Kastner, De Weerd, & Ungerleider, 2000; Schira, Fahle, Donner, Kraft, & Brandt, 2004). A large number of studies have been carried out on this area. Now it is believed that boundary detection is accomplished in primary visual cortex (Marcus & Van Essen, 2002; Rossi, Desimone, & Ungerleider, 2001; Zipser, Lamme, & Schiller, 1996), while surface segregation depends on feedback connection from temporal cortex to primary visual cortex (Heinen et al., 2005; Scholte et al., 2008). It is possible that the temporal cortex is more activated by "hole", thus surface segregation is facilitated, but boundary detection is not. So we suggest that temporal cortex is more activated by "hole", which could enhance the feedback connection to primary visual cortex and facilitate the processing of surface segregation (illustrated in Figure 1).

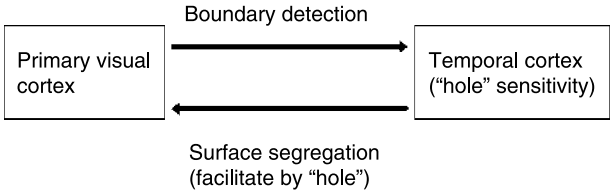

Figure 1. Paradigm of our suggestion: temporal cortex is "hole" sensitivity, thus facilitating the feedback connection to achieve surface segregation.

In order to test this hypothesis, backward masking paradigm was utilized in our research. Backward masking paradigm is widely used to study visual perception and awareness (Breitmeyer, Ro, & Ogmen, 2004; Enns & Di Lollo, 2000; Macknik, 2006). With masking effect, target stimulus is less visible. A large number of studies have focused on the neural basis of masking (Bacon-Macé, Macé, Fabre-Thorpe, & Thorpe, 2005; Breitmeyer et al., 2004; Enns & Di Lollo, 2000; Fahrenfort, Scholte, & Lamme, 2007; Lamme, Zipser, & Spekreijse, 2002; Macknik, 2006). There are different theories to explain the neural mechanisms of masking effect, including low-level lateral inhibition, high-level lateral inhibition, interchannel inhibition, and feedback connection disruption. Among these, feedback connection disruption was especially of interest in our research, because it suggested that backward masking interrupts the feedback connection in visual system, thus disturbs the visibility of the target (Fahrenfort et al., 2007). Deliberately, we could design an appropriate masking paradigm to produce the feedback disruption, meanwhile, to avoid other masking mechanism. According to our hypothesis, if feedback connection is interfered by masking, since temporal visual cortex is more activated by "hole", "hole" will be more visible than "no hole".

This paper aims to find out whether figures with "hole" and "no hole" are perceived differently during the figure–ground segmentation, especially at the process of surface segregation. By using backward masking paradigm that can disturb feedback connection, we expected that with the same masking condition, "hole" is easier perceived than "no hole".

Five experiments were carried out in this paper. The first fours were behavioral tests, and the last one was an ERP experiment. All the subjects were recruited from Yunnan

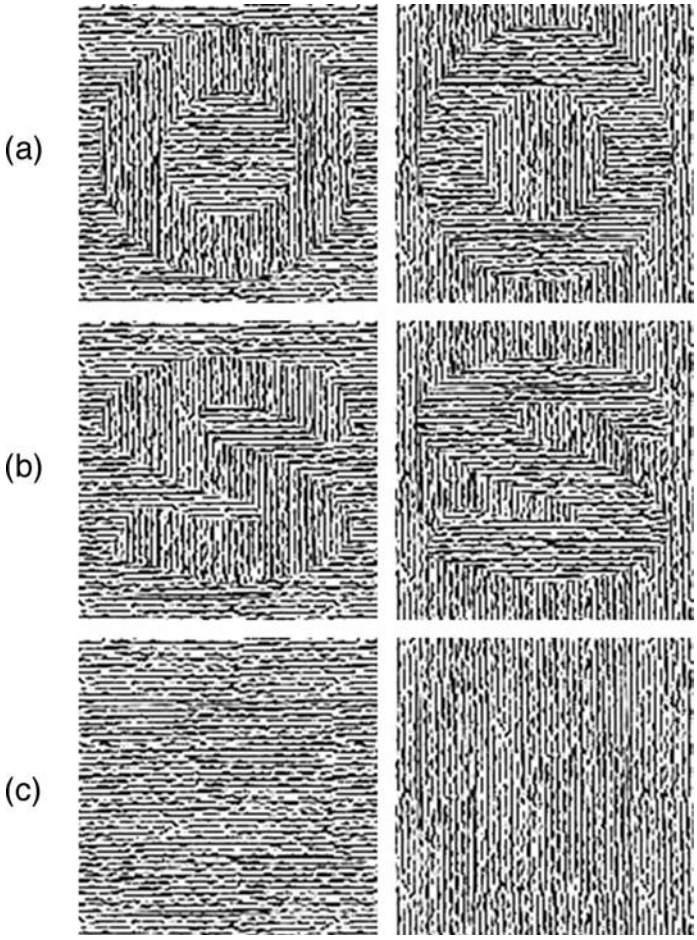

Figure 2. Three targets in Experiment 1. Each of which consists of two pictures: horizontal texture background and vertical texture background. (a) Ring. (b) S-like figure. (c) Homogeneous figure. In the following experiments, all the stimuli also consist of two pictures with different texture patterns.

University. They were paid to participate in these experiments. Each subject only participated in one of the experiments.

Experiment 1

In the present experiment, two figures were used: a ring ("hole") and an S-like figure ("no hole"). We expected that under the same masking effect, ring is more visible than S-like figure. Twelve undergraduates participated in this test.

Stimuli

Target stimuli consisted of orientation-defined texture figures of S-like figures, ring figures, and homogeneous patterns (see Figure 2). The original S-like and ring figures (2-D figures, obtained from Chen's laboratory) were designed to control for spatial frequency, luminous flux, perimeter length, and other possible confounds of local features (Chen, 2005). These characters remained the same after we converted them to texture figures. Each of the figures was a combination of horizontal texture-defined background and vertical texture-defined figure or vice versa. The texture figures were grayscale pictures consisted of noised oriented texture with a spatial frequency approximate 10 cycles/degree. The RNS visual contrasts of homogeneous figure, ring, and S-like figure were 43.33%, 44.17%, and 44.34%, respectively. The mask consisted of three white noise images, each of which was filtered at different spatial scales (see Figure 3b). The mask in this experiment was a randomized sequence of twelve images; each of the three different spatial filtered images being shown for four times. Every image was presented for 10 ms, so overall the masking stimulus lasted for 120 ms. This manipulation was to enhance the masking effect and to avoid a metacontrast relationship between targets and mask.

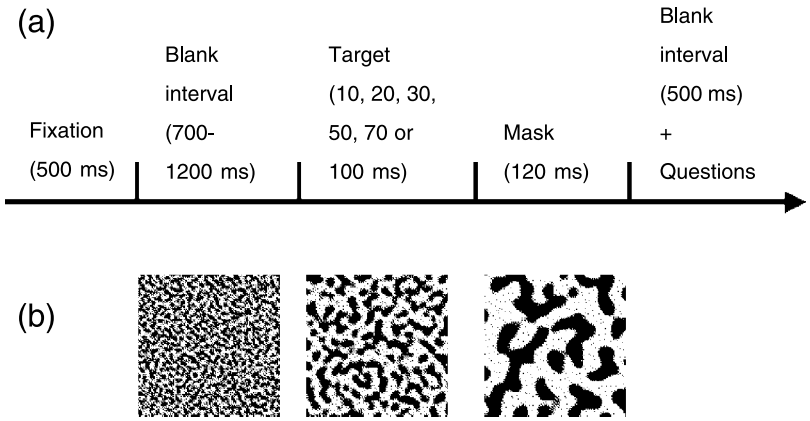

Figure 3. (a) Paradigm of a trial in Experiment 1. (b) The mask consists of three pictures; each was presented randomly for 10 ms, which together made a dynamic mask.

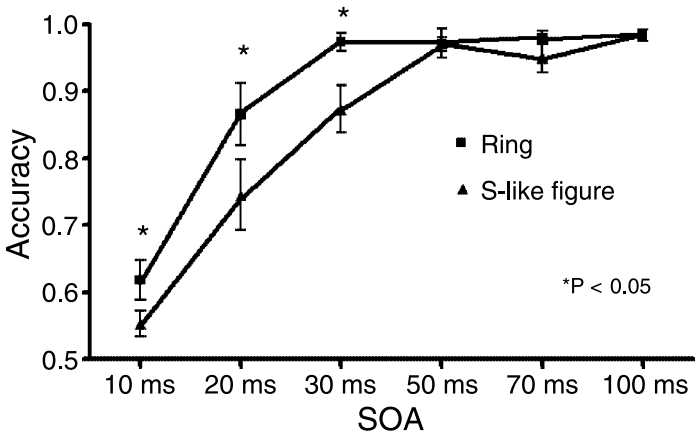

Figure 4. Behavioral results of Experiment 1. Within a certain SOA (≤30 ms), the visibility of ring is higher than S-like figure.

Procedure and task

Stimuli were presented on a 17-inch SVGA monitor (resolution of 1024 × 768, refresh rate of 100 Hz). Subjects were seated in front of the monitor with a view distance of 60 cm. The visual angle of both targets and masks was 10 degrees. Twelve blocks of 60 target/mask pairs were randomized within subjects. At the beginning of each trial, a fixation was displayed for 500 ms, and the subjects were asked to fixate. After an interval of 700–1200 ms (randomized for each trial) of blank screen, target was presented. The SOA between the targets and masks was manipulated between blocks (10, 20, 30, 50, 70, or 100 ms) randomly. Target duration was equivalent to the SOA. Mask was presented immediately following the offset of target (illustrated in Figure 3a). In half of the blocks (three out of six), thirty trials were S-like figures and thirty were blank patterns, in another half, thirty trials were ring figures and thirty trials were blank patterns. Subjects were asked to report whether a figure was presented or not by pressing two buttons of the mouse.

SOA	Figure	Accuracy	Mean difference (Ring − S)	Significance
10 ms	S	55.3%	6.5%	$P = 0.030$*
	Ring	61.8%		
20 ms	S	74.5%	12%	$P = 0.019$*
	Ring	86.5%		
30 ms	S	87.3%	10%	$P = 0.046$*
	Ring	97.3%		
50 ms	S	97.2%	0.2%	$P = 0.916$
	Ring	97%		
70 ms	S	95%	3%	$P = 0.095$
	Ring	98%		
100 ms	S	98.1%	0.2%	$P = 0.853$
	Ring	98.3%		

Table 1. The differences of visibility between ring and S-like figure at variant SOAs in Experiment 1.

Results

The behavioral performance of accuracy was analyzed by a MANOVA design for repeated measure and evaluated as a function of the duration of targets (see Figure 4). Greenhouse–Geisser correction was applied to the results. The accuracy was the averaged performance on both figure and homogeneous texture. The analyses on behavioral data in the following experiments also used the same statistical test method. For both S-like figure and ring, the accuracies decreased along with the decrease of SOA. At 10-, 20-, and 30-ms SOAs, the accuracies to detect a ring were significantly higher than S-like figure (see Table 1). These results supported our hypothesis that under the certain masking condition, "hole" (ring) is more visible than "no hole" (S-like figure). However, it is still possible that the difference of visibility in this experiment was caused by other feature differences, such as shape or the stimuli at the fovea. The next two experiments were to test this possibility.

Experiment 2

This experiment was to eliminate the possibility that different visibility between S-like figure and ring was caused by shape and other possible features. Another three figures were introduced in this experiment. Ten undergraduates participated in this test.

Methods

Five different targets were used in this experiment. They were S-like figure, ring, and other three 2-D figures, which are:

1. Orientation-defined texture pattern of disk (see Figure 5a): this one was used to eliminate the possibility that the difference is caused by shape. If so, disk figure that has a similar shape compared to ring should also be easier to detect than S-like figure.
2. Orientation-defined texture pattern of theta-like figure (see Figure 5b): since S-like figure has an oriented, straight-line segment in the middle, theta-like figure was designed to possess the same oriented line in the middle of the ring.

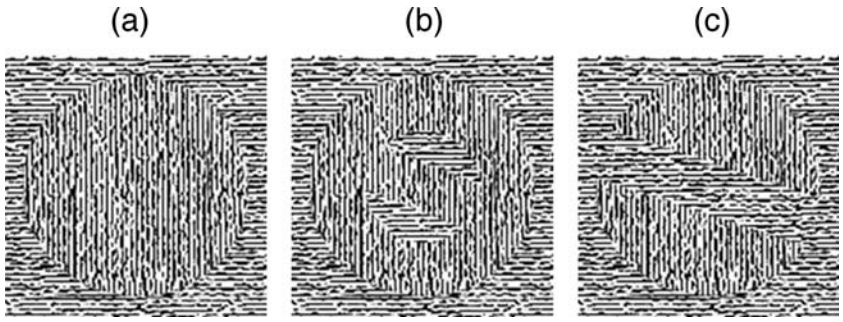

Figure 5. Three new targets used in Experiment 3. Only vertical texture figures were shown here. The contrasts of (a) disk, (b) theta-like, and (c) two-part figure are 44.29%, 44.15% and 44.28%, respectively.

3. Orientation-defined texture pattern of two-part figure (see Figure 5c): ring can be considered as two disks that overlapped, so the two-part figure was designed to testify whether the higher visibility of ring was caused by the number of figures.

The procedure and task were the same as in Experiment 1. The center of each target/mask pair was placed at the fixation. Three SOAs were chosen for this test: 10, 20, and 100 ms.

Results

Result was shown in Figure 6. At 100-ms SOA, all the five figures could be easily detected (accuracies above 93%). The accuracies decreased along with the decrease of the SOA. At 20-ms SOA, the detection of two-part, theta-like, and S-like figures was significantly less accurate than ring and theta-like figure (see Table 2). In this test, the accuracy to detect a disk was the same as an S-like figure, while smaller than a ring. So shape was not an issue to cause the different visibility between figures. Two-part figure was also more difficult to detect than ring, so the possibility that visibility difference was caused by number of figures was also eliminated. Theta-like figure was detected as easily as ring, so the straight line in the center (covers the fovea) is a reason to affect the visibility.

Experiment 3

This experiment was also to test whether the different visibility was caused by shape feature. Ten undergraduates participated in this test.

Methods

Three targets were used in this experiment. They were ring and two 2-D c-like figures: one was big c, which had the same area and perimeter length compared to ring, while the other was small c, which was 1/4 cutoff from the ring (see Figure 7a). The shapes of the two c-like figures were very similar to ring and could be considered as rings with a gap. On the other hand, c-like figures were "no-hole" figures and had different topological property compared to ring. The procedure and task were the same

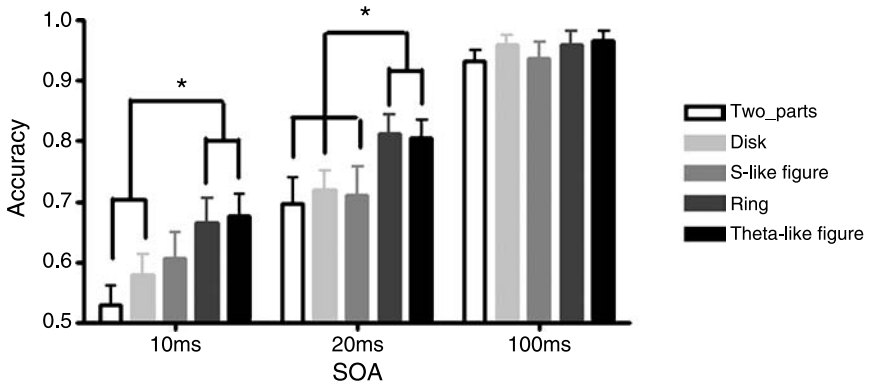

Figure 6. Behavioral results of Experiment 3. At 20-ms SOA, "hole" is more visible than "no hole".

Differences at 20-ms SOA	Two-part figure (accuracy: 69.7%)	Disk (accuracy: 72.1%)	S-like figure (accuracy: 71%)
Ring (accuracy: 81.1%)	MD = 11.5%, P = 0.030*	MD = 9.1%, P = 0.001*	MD = 10.2%, P = 0.016*
Theta-like figure (accuracy: 80.6%)	MD = 10.9%, P = 0.016*	MD = 8.5%, P = 0.001*	MD = 9.6%, P = 0.028*

Table 2. The differences of visibility between ring and S-like figure at 20-ms SOA in Experiment 3.

as in Experiment 1. The center of each target/mask pair was placed at the fixation. Three SOAs were chosen for this test: 10, 20, and 100 ms.

Results

Result was shown in Figure 7b. All the three figures could be easily detected at 100-ms SOA (accuracy above 94%). The accuracies decreased along with the decrease of the SOA. At both 10- and 20-ms SOA, the detection of big c and small c was significantly less accurate than ring (see Table 3). In this experiment, three figures had almost the same shape, except two c-like figures were "no hole" and ring was "hole". The result showed that ring was easier to be detected than c-like figures, thus indicated that the different visibility was sensitive to "hole" rather than the shape. However, according to the tolerance space (Chen, 2005), ring with a relatively small gap may also be perceived as a ring at first glance. Likewise in our experiment, the subjects reported sometimes that small c was perceived as a ring. Maybe it is the reason that when the SOA was 10 ms, the accuracy difference between small c and ring was just marginally significant (P = 0.081). However, if we amplify the gap of the ring, such as big c, it would not be perceived as ring (according to the reports of the subjects in the experiments), and the accuracy difference was significant ($P < 0.05$). Taking the results of this and the previous experiment, it was believable that topological difference of "hole" and "no-hole" figures was the only reason to induce the different visibility, rather than other feature differences.

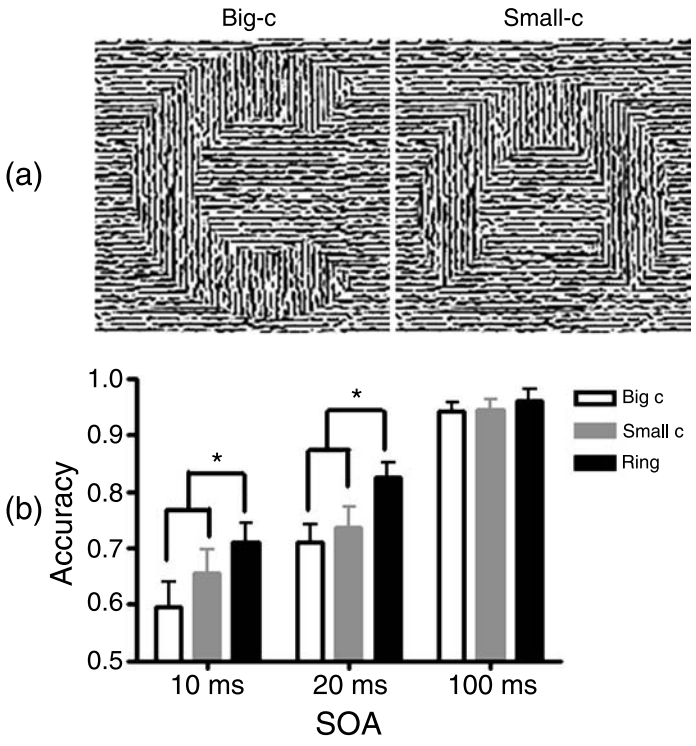

Figure 7. (a) The big-c and small-c figures in Experiment 3. The visual contrasts were 44.40% and 44.05% for big c and small c, respectively. (b) Behavioral results of Experiment 3. At mask condition, ring is more visible than both big-c and small-c figures.

Experiment 4

Other than ring and S-like figure, another group of pictures modified from Komatsu and Ideura's (1993) work was used in this experiment. This test was to illustrate that the different visibility between "hole" and "no hole" under certain masking condition was not particular for ring and S-like figure but was general for some similar figures. Fourteen undergraduates participated in this test.

Methods

In Komatsu's work, an IT neuron was found to be activated by "hole" (in their article named frame). So in this experiment, we utilized two groups of 2-D texture patterns modified from their work (see Figure 8). One group was "hole" pictures, another was "no-hole" pictures. The experimental paradigm was the same as Experiment 1. Two SOAs were selected as 20 and 100 ms.

Results

Results were shown in Figure 9. At 100-ms SOA, the two groups were easily detected without different visibility (accuracy above 94%). At 20-ms SOA, there was different visibility between the "hole" group and "no-hole" group, the accuracy of the former being significantly higher than the latter (see Table 4). This result was consistent with the previous experiments. So the different

SOA	Figure	Accuracy	Mean difference (Ring − c)	Standard error	Significance
10 ms	Ring	71.1%	–	–	–
	Big c	59.7%	11.5% (Ring − big c)	3.9%	$P = 0.017$
	Small c	65.6%	5.6% (Ring − small c)	2.8%	$P = 0.081$
20 ms	Ring	82.4%	–	–	–
	Big c	71.4%	11.3% (Ring − big c)	2.8%	$P = 0.003$
	Small c	73.6%	8.9% (Ring − small c)	2.8%	$P = 0.012$

Table 3. The differences of visibility between ring and c-like figures at variant SOAs in Experiment 3.

visibility between "hole" and "no hole" under masking conditions was general, not only for ring and S-like figure in particular.

Experiment 5

From the first four experiments, we testified our hypothesis with behavioral data. In this experiment, an ERP test was designed to find out the neural processing underlying the different visibility. Fifteen undergraduates participated in this test.

Methods

Experimental paradigm and stimuli were the same as in Experiment 1. Two SOAs were chosen as 20 and 100 ms. Previous results in Experiment 1 have shown that, at 20-ms SOA, masking could disturb the visibility of target, and accuracy at detecting ring was significantly higher than S-like figure. On the other hand, at 100-ms SOA, the masking effect hardly existed, because the visibilities of both ring and S-like figure were intact (accuracy above 98%). So in this experiment we utilized these two SOAs to study the neural mechanism of masking effect on ring and S-like figure.

Data acquisition and analysis

EEG data were recorded from 64 channels based on the international 10–20 system. Nose tip was used as reference electrode. Eye movements and blinks were monitored by electrodes placed near the outer canthus of each eye called horizontal electrooculograms (HEOG) and above and below the left eye called vertical electrooculograms (VEOG). The eye movements and blinks were recorded for ocular artifact reduction. Interelectrode impedance levels were kept below 5 kΩ. EEG was continuously recorded at a sampling rate of 1000 Hz during the experiment, using a band-pass filter of 0.05–100 Hz. ERPs were epoched for 200-ms pre-stimulus until 600-ms post-stimulus onset. Epochs contaminated with artifacts (threshold for artifact rejection was ±100 μV in all channels) were rejected before averaging.

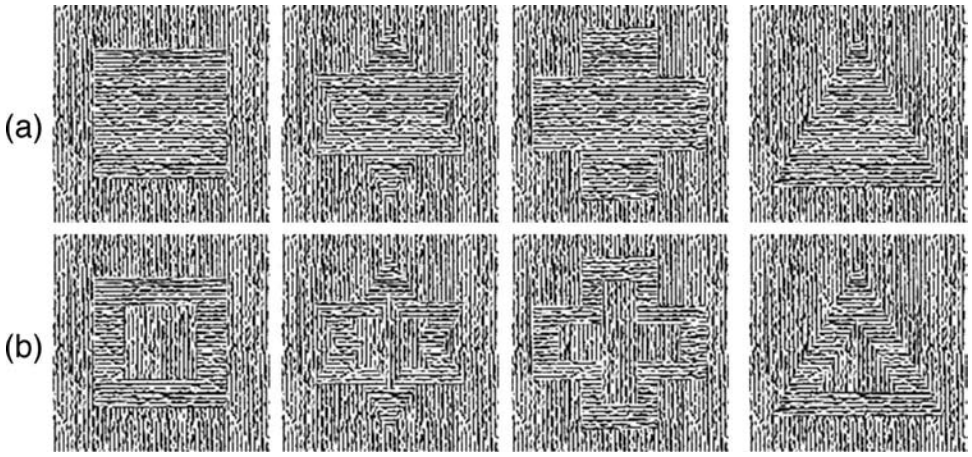

Figure 8. Targets used in Experiment 4. (a) "No-hole" group. (b) "Hole" group. Only horizontal texture figures were shown here. The mean contrasts of "no-hole" and "hole" groups were 44.41% and 44.33%, respectively.

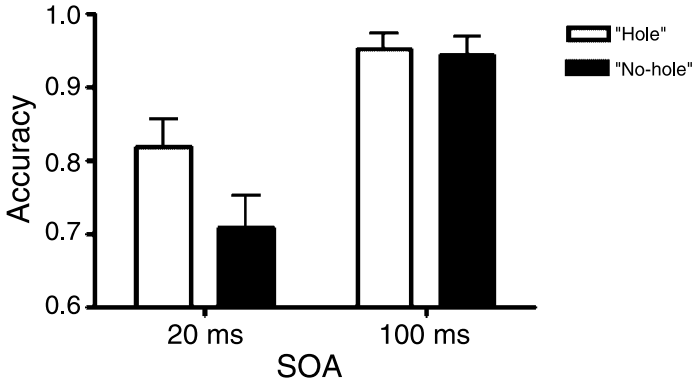

Figure 9. Behavioral results of Experiment 4. At 20-ms SOA, "hole" is more visible than "no hole".

Results

Behavioral accuracy was similar to the results in Experiment 1. Under masking condition (20-ms SOA), there is significant difference ($P < 0.001$) of accuracies between ring (74.9%) and S-like figure (67.9%). While under non-masking condition (100-ms SOA), there is no difference; the accuracy for ring and S-like figure was 99.6% and 99.8%, respectively.

Texture segregation ERP (tsERP) was analyzed in this test. It has been used to study the figure–ground segregation. tsERP is defined as a different wave by subtracting homogeneous figure from segregated figure. This subtraction can eliminate the "low-level VEP" evoked by the onset of the local feature elements and reserve the information of texture segregation (Bach & Meigen, 1998). The latencies of the components of tsERP differ between studies, varying from approximately 90 ms to after 250 ms (Caputo & Casco, 1999; Heinrich, Andrés, & Bach, 2007; Lamme, Rodriguez-Rodriguez, & Spekreijse, 1999; Scholte et al., 2008).

In order to test at which time points the tsERP components significantly deflect from chance, the analysis was performed by a paired two-tailed t-test at each time point of tsERPs between 0 and 300 ms. Because there were 15 subjects that participated in this test, so at time point p, the tsERP was significant when the t-value of p was larger than 2.145 ($t(14) = 2.145$, $p = 0.05$). So tsERP components consisted of the time points (at least 10 consecutive points) whose t-values were larger than 2.145. Figure 10 showed the ERPs of four conditions (two figures, two SOAs) recorded from two areas (temporal-occipital lobe and occipital lobe). In each condition, figure-target evoked ERP and homogeneous-target evoked ERP were presented. tsERP was represented as the difference between two ERPs. For each condition, different tsERP components were presented in Table 5. There were two tsERP components for S-like figure in both masking and non-masking conditions. The onset of the first components appeared at around 80 ms for both SOAs, while the onset of the second appeared at 138 and 162 ms for masking and non-masking conditions, respectively. However, for ring figure, there is only one significant component; the onset appeared at 142 and 150 ms for masking and non-masking conditions, respectively.

SOA	Figure	Accuracy	Mean difference	Significance
20 ms	"No hole"	70.7%	11.1%	$P = 0.004$*
	"Hole"	81.8%		
100 ms	"No hole"	94.4%	0.8%	$P = 0.791$
	"Hole"	95.2%		

Table 4. The differences of visibility between "hole" and "no hole" at variant SOA in Experiment 4.

The tsERPs (different waves) were also shown in Figure 11. The scalp distributions of the two tsERP components were shown in Figure 12. The time interval of the first component was started at 75 ms and ended at 100 ms. This interval was selected based on the significant paired t-test results (see Table 5). The second component was started at 140 ms and ended at 200 ms; 140 ms was chosen because it was the onset latency of the second component (see Table 5); 200 ms was chosen as the limitation to prevent some later complex perceptual processing would influence the tsERP of figure–ground segregation (more detailed reason was to be explicated in the Discussion section). From the tsERPs and scalp distributions (Figures 11 and 12), it was clearly shown that the first tsERP component was not interfered by masking effect, for both ring and S-like figure. However, the second tsERP component was interfered by masking effect. For ring, the second component was reduced but can still be observed in masking condition. On the other hand, for S-like figure, the second component almost vanished.

Quantification of the mean amplitudes of two tsERP components was analyzed by a MANOVA design for repeated measure. The first one was the tsERP component that appeared on S-like figure around 80 ms. Area report of tsERP between 75 and 100 ms was analyzed with three factors: brain area (temporal-occipital area including PO7 and PO8, occipital area including OZ and POZ), SOA (masking condition and non-masking condition), and figure (ring and S-like figure). Greenhouse–Geisser correction was applied to the results. The main effect of figure was significant ($F = 9.212$, $P = 0.009$), 0.046 μV and 1.148 μV for ring and S-like figure, respectively. There is no significant difference of the main effect of SOA and brain area. In addition, there is no interaction effect in this analysis. For S-like figure, the first tsERP component did not show significant difference ($F = 0.086$, $P = 0.774$) between masking and non-masking conditions. For ring, although there is no significant tsERP component pre-100 ms, the mean amplitude of tsERPs also did

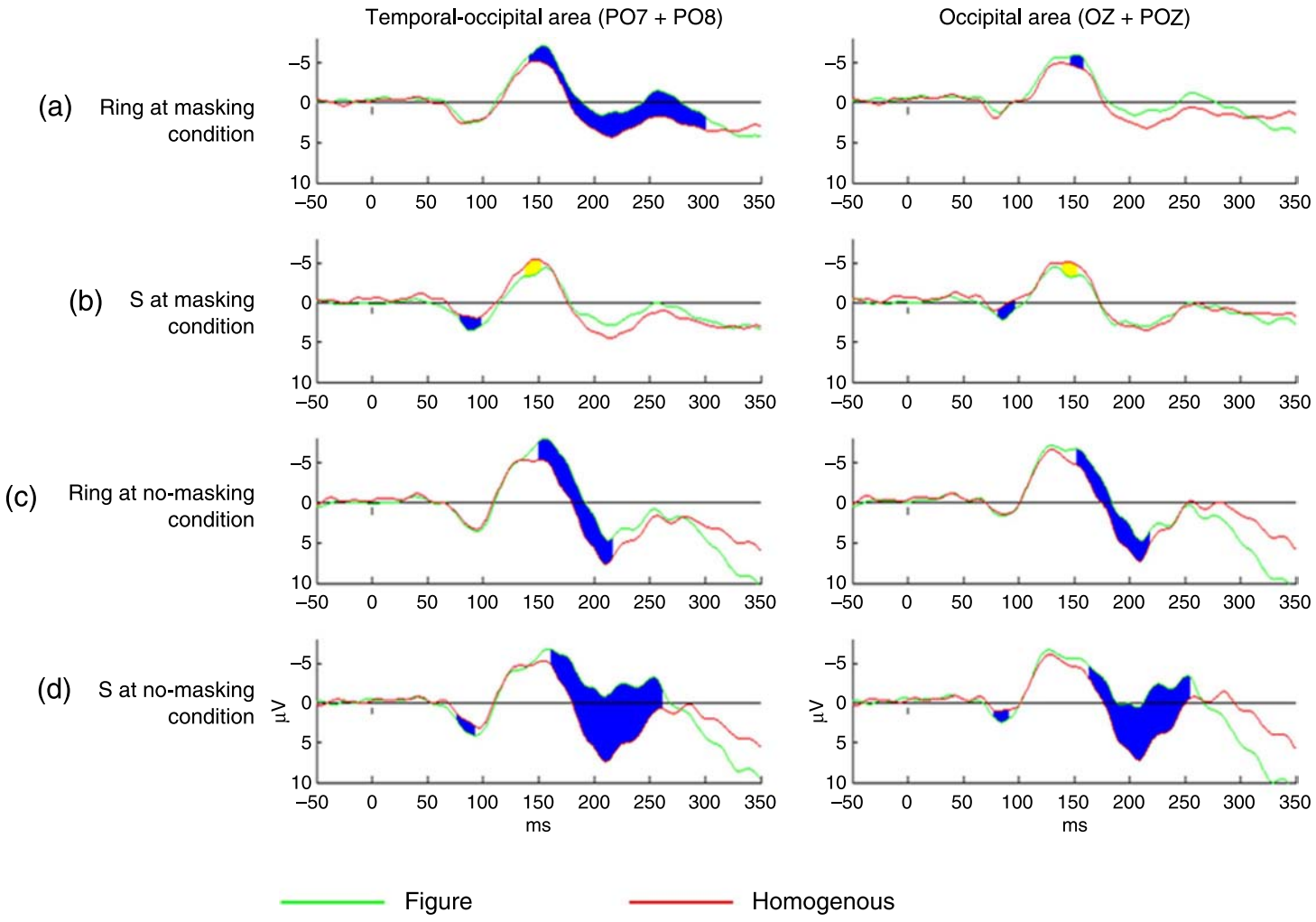

Figure 10. Green and red lines represented figure and homogeneous ERPs, respectively. Their subtraction depicted the tsERPs. Blue and yellow areas represented the significant difference of two ERPs with paired *t*-test between 0 and 300 ms. Blue area represented a negative component of tsERP, while yellow area represented a positive component.

not show significant difference ($F = 0.453$, $P = 0.512$) between masking and non-masking conditions.

Analysis on the second tsERP component was limited in the time window of 140–200 ms. In addition, MANOVA design was analyzed with three factors: brain area, SOA, and figure. The main effect of SOA was significant ($F = 15.474$, $P = 0.001$), -0.608 μV and -2.828 μV for masking and non-masking conditions, respectively. There is no significant difference of the main effect of brain area and figure. The interaction effect of figure and SOA showed a significant difference ($F = 10.457$, $P = 0.006$). Specifically, for ring condition, the tsERPs between different SOAs did not show significant difference. On the other hand, for S-like figure condition, the tsERP showed significant difference ($F = 21.317$, $P < 0.001$), 0.262 μV and -3.202 μV for masking and non-masking conditions, respectively.

Correlation between the mean amplitudes of tsERP components and behavioral accuracies was calculated in masking conditions and found a between-subject effect. Pearson correlation was analyzed and found that the second tsERP components were correlated with the accuracies of both ring ($r = -0.700$, $p = 0.004$) and S-like figure ($r = -0.700$, $p = 0.004$). On the other hand, there is no correlation of the first tsERP components with both ring

	Temporal-occipital area	Occipital area
Ring at masking condition	–	–
	142–300 ms	140–158 ms
S at masking condition	80–97 ms	82–96 ms
	138–151 ms	140–152 ms
Ring at non-masking condition	–	–
	150–216 ms	153–217 ms
S at non-masking condition	77–92 ms	78–90 ms
	162–216 ms	164–254 ms

Table 5. The time course of significant tsERP components that appeared in each condition at two different brain areas.

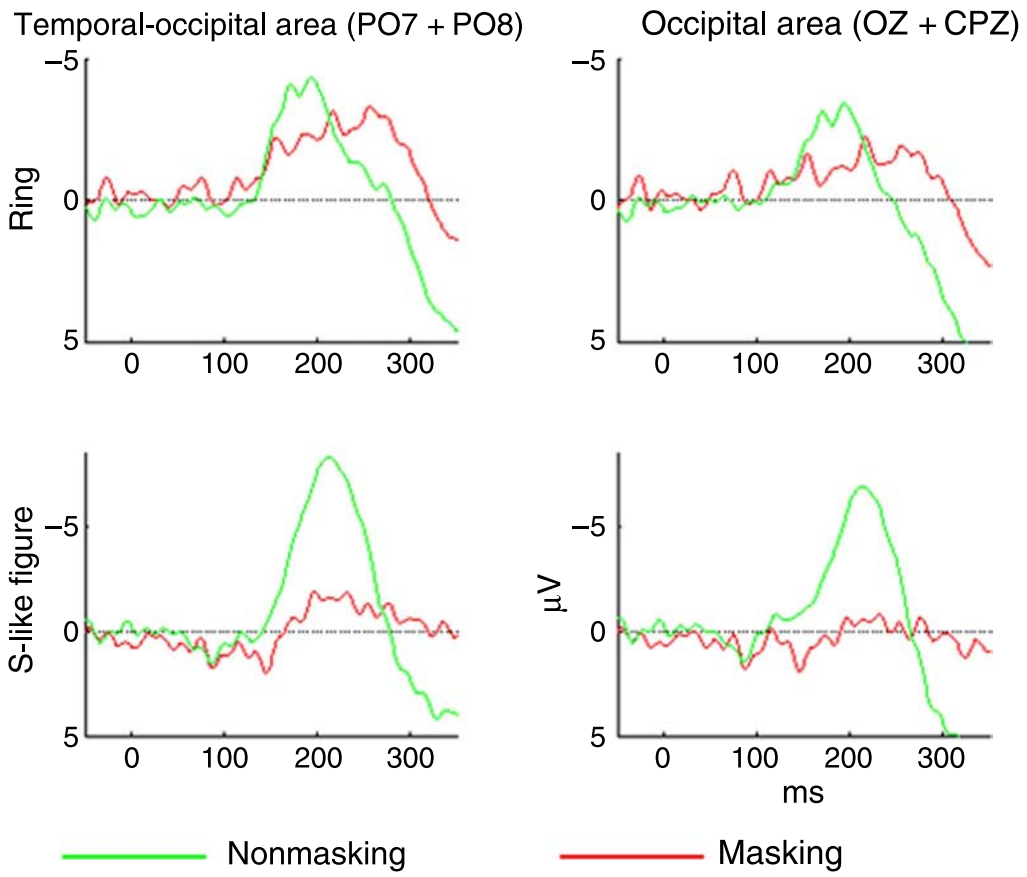

Figure 11. The different waves (tsERP components) of ring and S-like figure in both masking and non-masking conditions, at temporal-occipital and occipital areas. Green and red lines represent non-masking and masking conditions, respectively.

(r = 0.027, p = 0.923) and S-like figure (r = 0.280, p = 0.312). The correlations were shown in Figure 13. The correlations in non-masking condition were not analyzed because of the ceiling effect of behavioral accuracies.

Discussion

This paper demonstrated the different masking effects between "hole" and "no hole". Experiment 1 suggested that the visibility of ring was higher than S-like figure under the same masking effect. Experiments 2 and 3 indicated that rather than other feature differences, topological (hole vs. no hole) difference was the only reason to cause the different visibility. Experiment 4 utilized another group of "hole" and "no-hole" figures to confirm the above results. That is, under certain masking effect, "hole" can be easier detected than "no hole".

As Chen (2005) has proposed, there seem to be, in principle, no two geometric features that differ only in topological properties. In our experiments, there are also other differences between "hole" and "no hole" besides topology, and it is inevitable. So several experiments were carried out, maybe in one experiment there are some other features that were not well controlled, but they could be controlled in other experiments. All of these experiments together could demonstrate that the visibility under masking condition is "hole" sensitivity, rather than other local feature sensitivity.

Experiment 5 was an ERP test to find the neural mechanism for the different visibilities. tsERP was analyzed and two components were obtained, one appearing around 80 ms and a subsequent one around 140 ms. The two tsERP components were also reported in previous studies. In Scholte et al. (2008), by applying spline Laplacian, the two appeared at 92 ms and 140 ms, respectively. In Heinrich et al. (2007), the two appeared at 110 ms and 230 ms, respectively. In Caputo and Casco (1999), relatively later components were shown at 140–160 ms and 200–260 ms, respectively. Consistently, unit recording on monkey also demonstrated these two components occurring at 90 ms and 120 ms (Lamme et al., 1999). It was widely regarded that the two components represented boundary detection and surface segregation, respectively. We believe that the two components in our results also represented boundary detection and surface segregation, respectively, which will be explicated as follows:

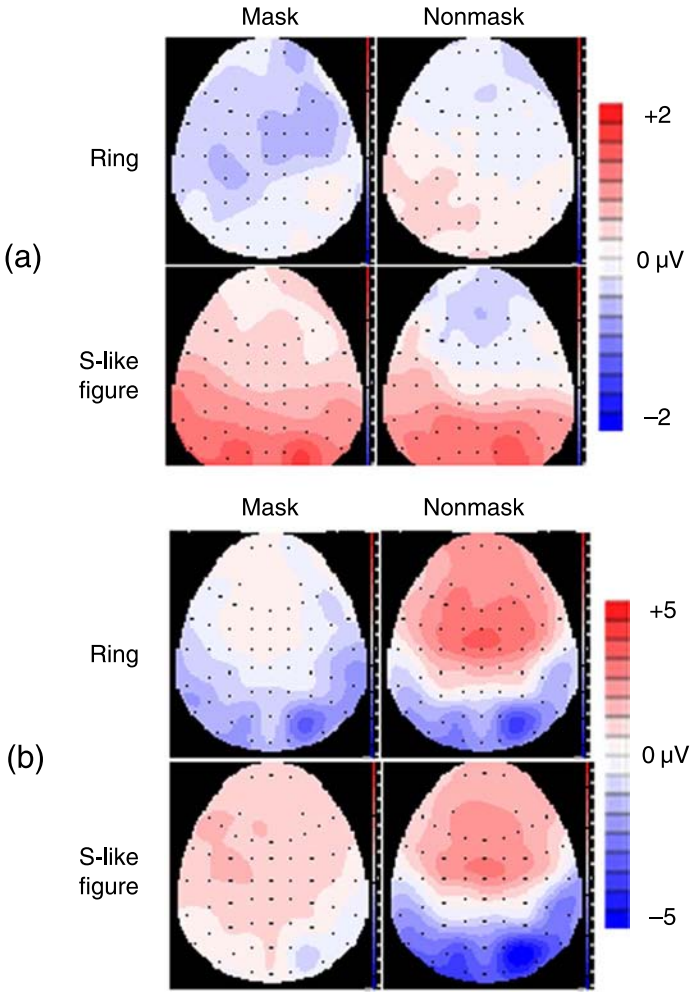

Figure 12. Scalp distributions of the two tsERP components. (a) The first tsERP component. (b) The second tsERP component.

1. The time course of the first tsERP component in our results was consistent with the previous findings. Furthermore, according to Fahrenfort et al. (2007), boundary detection was not affected by backward masking. Consistently, the first tsERP component in our results was also intact under masking condition. Specifically, for S-like figure, the first tsERP component did not show any differences in masking or non-masking condition. On the other hand, for the ring figure, though there is no significant tsERP component in this time window (around 90 ms), the mean amplitude of tsERP still did not show any difference between masking and non-masking conditions. So, it is believable that the first tsERP represented the processing of boundary detection.
2. Similarly, we believe that the second tsERP component appearing around 140 ms represented the surface segregation. First, its time course was consistent with other results of ERP and unit recording studies. Second, in masking condition, the overall tsERP component was smaller compared with unmasking condition. This was consistent with the neural mechanism study on backward masking (Fahrenfort et al., 2007). Furthermore, this tsERP component had a positive correlation with the visibility under masking effect. Similar correlations were also obtained in previous tsERP studies (Bach & Meigen, 1998; Haynes et al., 2005). This correlation indicated that the second tsERP component reflected the salience of the perception of the target. It is common sense that feedback connection is crucial for conscious perception (Bacon-Macé et al., 2005; Haynes et al., 2005; Ro, Breitmeyer, Burton, Singhal, & Lane, 2003). In addition, it is believed that surface segregation depends on this feedback connection (Scholte et al., 2008). Taking together, we believe that the second tsERP component was caused by feedback connection and represented the surface segregation.

Thus, at the stage of boundary detection, the tsERP components of both ring and S-like figure were intact under masking effect. It indicated that feedforward connection in visual ventral pathway was not disturbed by backward masking. However, at the stage of surface segregation, the tsERP of S-like figure was interfered by the masking effect, while the tsERP of ring was not. It suggested that feedback connection for "hole" seems more stable compared to "no hole". In another fMRI study (Vinberg & Grill-Spector, 2008), it is found that lateral occipital complex (LOC) responded strongly to holes than to global surface; however, no such result in temporal cortex or primary visual cortex was observed. From our ERP data, it is hard to tell the exact visual area that responded strongly to "hole" than "no hole", but according to previous literatures (Komatsu & Ideura, 1993; Wang et al., 2007; Zhuo et al., 2003), it is more likely that temporal cortex responded strongly to "hole", thus facilitating the formation of surface segregation. However, it is still possible that other higher visual cortex (such as LOC) in ventral pathway also responded strongly to "hole".

There are several theories to explain the neural mechanism of backward masking effect (Bachmann, Luiga, & Põder, 2005). However, in our results, rather than other reasons, feedback connection was the most important one to disturb the visibility. The target figures used in our results were second-order stimuli (orientated texture-defined patterns), and dynamic masks were designed to avoid a metacontrasting relation to the target. So the masking effect should not be due to low-level lateral inhibition. In addition, high-level lateral inhibition and interchannel inhibition could hardly be the reason to explain our data (this has been discussed explicitly in Fahrenfort et al., 2007). Our data can be explained well by the theory that backward masking disrupts feedback connection while feedforward connection is intact. However, it is still possible that in our experiment, masking effect was somehow affected by lateral inhibition, but mainly it counts on disrupting feedback connections in visual system.

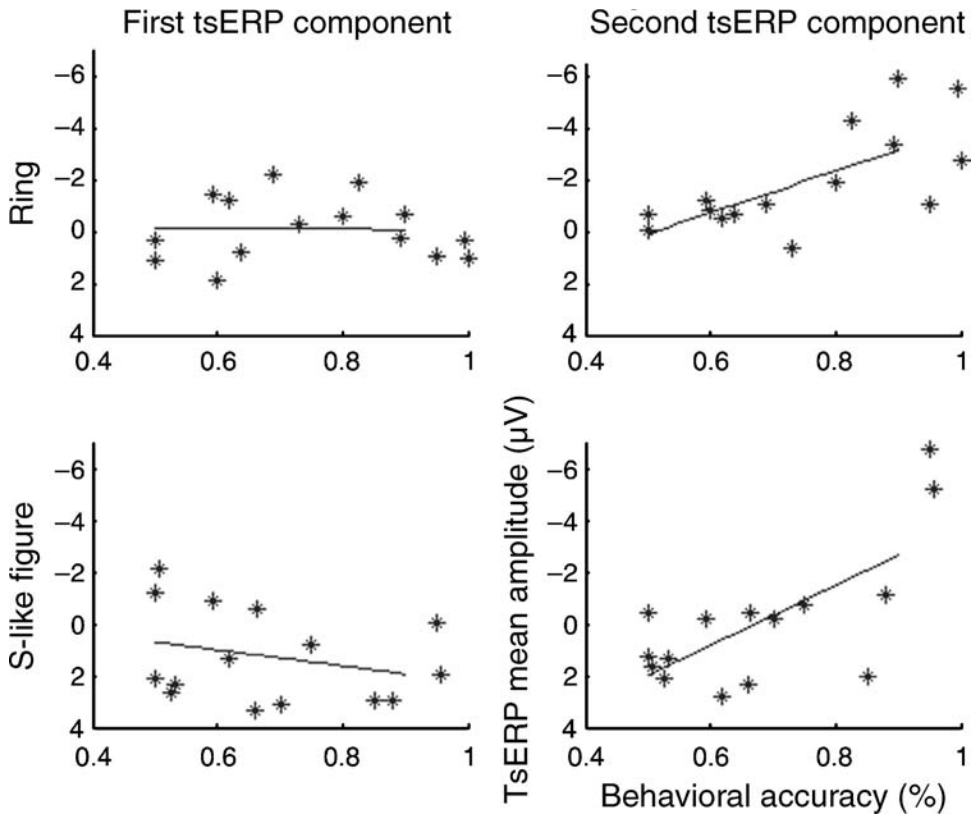

Figure 13. The correlations of tsERP components and behavioral accuracies in masking condition.

In this study, we limited the second tsERP component in a time window preceding 200 ms, in case that some complex perceptual processing would influence the tsERP of figure–ground segregation. In another VEP study utilizing passive paradigm without masking, we obtained a similar result that "no hole" elicits a larger N1 than "hole" (unpublished data), which may be caused by some perceptual processing after surface segregation. In the experiments of this paper, in non-masking condition, though it did not show a significant difference (F = 14.000, P = 0.266), the mean amplitude of the second tsERP component of S-like figure (−3.202 μV) was larger than ring (−2.455 μV). This may be also caused by the mix-up of later complex perception processing.

The first tsERP component, which reflects the process of boundary detection, was not correlated with the visibility under masking condition. It indicated that in our experiments, the local features of edges did not affect the figure–ground segregation task. At temporal visual area, local features were integrated into global features, and at this time the "hole" sensitivity appeared. The evidence is that the second tsERP components were correlated with the visibilities of both ring and S-like figure. So essentially, it is that the way how edges integrated (into global features) caused the different visibility, rather than the local features of edges.

Our experiments verified our hypothesis that temporal visual area is more activated by "hole" stimuli, thus facilitating the feedback connection in the ventral visual system. It is not clear whether topological perception totally relies on the sensitivity to "hole". One of the topological differences is caused by the presence or absence of a visual stimulus. For example, in our study, S-like figure and homogenous figure are also different in terms of topology. However, we can still explain this kind of topological difference in terms of "hole", because one can consider S-like figure as an S-like hole when you take the background texture as a figure. On the other hand, homogenous figure can be considered as a textured figure without any holes. In this way, the presence or absence of a visual stimulus can be also considered as the presence or absence of a hole. In addition, it should be noted that we concentrated only on the difference between "hole" and "no hole". It is still unclear as to the neural mechanism between perceiving figures with different numbers of holes. So further research should be focused on whether all topological perception can be explained by the sensitivity to "hole" and the numbers of "hole".

Acknowledgments

This research was supported by the Ministry of Science and Technology of China Grant 2005CB522800, the High Technology Research and Development Program of China

(2006AA01Z129), and the Research Fund of Yunnan University (KL080012).

Commercial relationships: none.
Corresponding author: Yuanye Ma.
Email: yuanma0716@vip.sina.com.
Address: Kunming Institute of Zoology, China Academy of Sciences, Kunming, China.

References

Altmann, C. F., Bülthoff, H. H., & Kourtzi, Z. (2003). Perceptual organization of local elements into global shapes in the human visual cortex. *Current Biology, 13,* 342–349. [PubMed] [Article]

Appelbaum, L. G., Wade, A. R., Vildavski, V. Y., Pettet, M. W., & Norcia, A. M. (2006). Cue-invariant networks for figure and background processing in human visual cortex. *Journal of Neuroscience, 26,* 11695–11708. [PubMed] [Article]

Bach, M., & Meigen, T. (1992). Electrophysiological correlates of texture segregation in the human visual evoked potential. *Vision Research, 32,* 417–424. [PubMed]

Bach, M., & Meigen, T. (1998). Electrophysiological correlates of human texture segregation, an overview. *Documentary Ophthalmology, 95,* 335–347. [PubMed]

Bachmann, T., Luiga, I., & Põder, E. (2005). Variations in backward masking with different masking stimuli: II. The effects of spatially quantised masks in the light of local contour interaction, interchannel inhibition, perceptual retouch, and substitution theories. *Perception, 34,* 139–153. [PubMed]

Bacon-Macé, N., Macé, M. J., Fabre-Thorpe, M., & Thorpe, S. J. (2005). The time course of visual processing: Backward masking and natural scene categorisation. *Vision Research, 45,* 1459–1469. [PubMed]

Breitmeyer, B. G., Ro, T., & Ogmen, H. (2004). A comparison of masking by visual and transcranial magnetic stimulation: Implications for the study of conscious and unconscious visual processing. *Conscious Cognitive, 13,* 829–843. [PubMed]

Caputo, G., & Casco, C. (1999). A visual evoked potential correlate of global figure–ground segmentation. *Vision Research, 39,* 1597–1610. [PubMed]

Casati, R. (2009). Does topological perception rest on a misconception about topology? *Philosophical Psychology, 22,* 77–81.

Chen, L. (1982). Topological structure in visual perception. *Science, 218,* 699–700. [PubMed]

Chen, L. (2005). The topological approach to perceptual organization. *Visual Cognition, 12*, 553–701.

Chen, L., Zhang, S., & Srinivasan, M. V. (2003). Global perception in small brains: Topological pattern recognition in honey bees. *Proceedings of the National Academy of Sciences of the United States of America, 100*, 6884–6889. [PubMed] [Article]

Enns, J. T., & Di Lollo, V. (2000). What's new in visual masking? *Trends in Cognitive Sciences, 4*, 345–352. [PubMed]

Fahrenfort, J. J., Scholte, H. S., & Lamme, V. A. (2007). Masking disrupts reentrant processing in human visual cortex. *Journal of Cognitive Neuroscience, 19*, 1488–1497. [PubMed]

Haynes, J. D., Driver, J., & Rees, G. (2005). Visibility reflects dynamic changes of effective connectivity between V1 and fusiform cortex. *Neuron, 46*, 811–821. [PubMed] [Article]

Heinen, K., Jolij, J., & Lamme, V. A. (2005). Figure–ground segregation requires two distinct periods of activity in V1: A transcranial magnetic stimulation study. *Neuroreport, 16*, 1483–1487. [PubMed]

Heinrich, S. P., Andrés, M., & Bach, M. (2007). Attention and visual texture segregation. *Journal of Vision, 7*(6):6, http://journalofvision.org/7/6/6/, doi:10.1167/7.6.6. [PubMed] [Article]

Kastner, S., De Weerd, P., & Ungerleider, L. G. (2000). Texture segregation in the human visual cortex: A functional MRI study. *Journal of Neurophysiology, 83*, 2453–2457. [PubMed] [Article]

Komatsu, H., & Ideura, Y. (1993). Relationships between color, shape, and pattern selectivities of neurons in the inferior temporal cortex of the monkey. *Journal of Neurophysiology, 70*, 677–694. [PubMed]

Lamme, V. A., Rodriguez-Rodriguez, V., & Spekreijse, H. (1999). Separate processing dynamics for texture elements, boundaries and surfaces in primary visual cortex of the macaque monkey. *Cerebral Cortex, 9*, 406–413. [PubMed] [Article]

Lamme, V. A., Zipser, K., & Spekreijse, H. (2002). Masking interrupts figure–ground signals in V1. *Journal of Cognitive Neuroscience, 14*, 1044–1053. [PubMed]

Macknik, S. L. (2006). Visual masking approaches to visual awareness. *Progress in Brain Research, 155,* 177–215. [PubMed]

Marcus, D. S., & Van Essen, D. C. (2002). Scene segmentation and attention in primate cortical areas V1 and V2. *Journal of Neurophysiology, 88*, 2648–2658. [PubMed] [Article]

Pomerantz, J. R. (2003). Wholes, holes, and basic features in vision. *Trends in Cognitive Sciences, 7*, 471–473. [PubMed]

Ren, P., Meng, Q. L., Wang, B., Liu, L. J., Hu, X. T., Ma, Y. Y., et al. (2007). Topological perception of Amblyopic Subjects. *Progress in Biochemistry and Biophysics, 34,* 127.

Ro, T., Breitmeyer, B., Burton, P., Singhal, N. S., & Lane, D. (2003). Feedback contributions to visual awareness in human occipital cortex. *Current Biology, 13*, 1038–1041. [PubMed] [Article]

Rossi, A. F., Desimone, R., & Ungerleider, L. G. (2001). Contextual modulation in primary visual cortex of macaques. *Journal of Neuroscience, 21*, 1698–1709. [PubMed] [Article]

Schira, M. M., Fahle, M., Donner, T. H., Kraft, A., & Brandt, S. A. (2004). Differential contribution of early visual areas to the perceptual process of contour processing. *Journal of Neurophysiology, 91*, 1716–1721. [PubMed] [Article]

Scholte, H. S., Jolij, J., Fahrenfort, J. J., & Lamme, V. A. (2008). Feedforward and recurrent processing in scene segmentation: Electroencephalography and functional magnetic resonance imaging. *Journal of Cognitive Neuroscience, 20*, 2097–2109. [PubMed]

Thielscher, A., Kölle, M., Neumann, H., Spitzer, M., & Grön, G. (2008). Texture segmentation in human perception: A combined modeling and fMRI study. *Neuroscience, 151*, 730–736. [PubMed]

Vinberg, J., & Grill-Spector, K. (2008). Representation of shapes, edges, and surfaces across multiple cues in the human visual cortex. *Journal of Neurophysiology, 99*, 1380–1393. [PubMed] [Article]

Wang, B., Zhou, T. G., Zhuo, Y., & Chen, L. (2007). Global topological dominance in the left hemisphere. *Proceedings of the National Academy of Sciences of the United States of America, 104*, 21014–21019. [PubMed] [Article]

Zhuo, Y., Zhou, T. G., Rao, H. Y., Wang, J. J., Meng, M., Chen, M., et al. (2003). Contributions of the visual ventral pathway to long-range apparent motion. *Science, 299*, 417–420. [PubMed]

Zipser, K., Lamme, V. A., & Schiller, P. H. (1996). Contextual modulation in primary visual cortex. *Journal of Neuroscience, 16*, 7376–7389. [PubMed] [Article]